International Journal of Pharmaceutics 375 (2009) 75–83

Contents lists available at ScienceDirect

International Journal of Pharmaceutics

journal homepage: www.elsevier.com/locate/ijpharm

Design, preparation, *in vitro* and *in vivo* evaluation of ^{99m}Tc-N_2S_2-Tat(49–57)-bombesin: A target-specific hybrid radiopharmaceutical

Clara L. Santos-Cuevas[a,b], Guillermina Ferro-Flores[a,*], Consuelo Arteaga de Murphy[c], Flor de M. Ramírez[a], Myrna A. Luna-Gutiérrez[a,b], Martha Pedraza-López[c], Rocío García-Becerra[c], David Ordaz-Rosado[c]

[a] *Instituto Nacional de Investigaciones Nucleares, Mexico*
[b] *Universidad Autónoma del Estado de México, Mexico*
[c] *Instituto Nacional de Ciencias Médicas y Nutrición Salvador Zubirán, Mexico*

ARTICLE INFO

Article history:
Received 24 December 2008
Received in revised form 11 April 2009
Accepted 14 April 2009
Available online 22 April 2009

Keywords:
Radiolabeled bombesin
Hybrid radiopharmaceutical
Peptide-receptor imaging
Tat-bombesin

ABSTRACT

The gastrin-releasing peptide receptor (GRP-r) is over-expressed in various human tumors. Recently, ^{99m}Tc-EDDA/HYNIC-Lys^3-bombesin (^{99m}Tc-BN) was reported as a radiopharmaceutical with specific cell GRP-r binding and images in breast cancer patients demonstrated distinct radioactivity accumulation in malignant tissue. The HIV Tat-derived peptide has been used to deliver a large variety of cargoes into cells. Therefore, a new hybrid radiopharmaceutical of type ^{99m}Tc-N_2S_2-Tat(49–57)-Lys^3-bombesin (^{99m}Tc-Tat-BN) would increase cell uptake. The aim of this research was to prepare and assess *in vitro* and *in vivo* uptake kinetics in cancer cells of ^{99m}Tc-Tat-BN and to compare its cellular internalization with that of ^{99m}Tc-BN. Structures of N_2S_2-Tat-BN and Tc(O)N_2S_2-Tat-BN were calculated by an MM procedure. ^{99m}Tc-Tat-BN was synthesized and stability studies carried out by HPLC and ITLC-SG analyses in serum and cysteine solutions. *In vitro* internalization was tested using human prostate cancer PC-3 cells and breast carcinoma cell lines MDA-MB231 and MCF7. Biodistribution was determined in PC-3 tumor-bearing nude mice. Results showed a minimum energy of 271 kcal/mol for N_2S_2-Tat-BN and 300 kcal/mol for Tc(O)N_2S_2-Tat-BN. ^{99m}Tc-Tat-BN radiochemical purity was >90%. *In vitro* studies demonstrated stability in serum and cysteine solutions, specific cell receptor binding and internalization in three cell lines was significantly higher than that of ^{99m}Tc-BN ($p < 0.05$). The tumor-to-muscle radioactivity ratio was 8.5 for ^{99m}Tc-Tat-BN and 7 for ^{99m}Tc-BN. Therefore, this hybrid is potentially useful in breast and prostate cancer imaging.

1. Introduction

Molecular imaging is defined as the visualization, characterization and measurement of biological processes at the molecular and cellular levels in humans and other living systems (Thakur and Lentle, 2005). Cancer imaging techniques using radiotracers targeted to specific receptors have yielded successful results demonstrating the utility of such approaches for developing specific radiopharmaceuticals.

Regulatory peptide receptors are over-expressed in numerous human cancer cells. These receptors have been used as molecular targets for radiolabeled peptides to localize cancer tumors. The useful clinical results achieved during the last decade with somatostatin receptor-expressing neuroendocrine tumor imaging, have been extended to the study of other radiopeptides to target alternative cancer-associated peptide receptors such as gastrin-releasing peptide, cholecystokinin, peptide ligands for integrin receptors or neurotensin. The improvement of radiopeptide analogues allows specific clinical imaging of different tumor types, including breast, prostate, intestine, pancreas and brain tumors (Ferro-Flores et al., 2006a; de Visser and Verwijnen, 2008).

The bombesin (BN) peptide was isolated from frog skin and belongs to a large group of neuropeptides with many biological functions. The human equivalent is the gastrin-releasing peptide (GRP, 27 amino acids) and its receptors (GRP-r) are over-expressed in the tumor cell membrane in an early stage of carcinogenesis (Lui et al., 2003). GRP and BN differ by only 1 of 10 carboxy-terminal residues and this explains the similar biological activity of the two peptides (Reubi, 2003). The strong-specific BN–GRP-r binding is the basis for labeling BN with radionuclides (Baidoo et al., 1998; La Bella et al., 2002; Varvarigou et al., 2002; Smith et al., 2003; Faintuch et al., 2005; Nock et al., 2005; Lin et al., 2005; Alves et al., 2006; Zhang et al., 2006a; Garcia-Garayoa et al., 2007; Kunstler et al., 2007).

^{99m}Tc-EDDA/HYNIC-Lys^3-BN (^{99m}Tc-BN) obtained from lyophilized kit formulations has been reported as a radiopharma-

* Corresponding author at: Departamento de Materiales Radiactivos, Instituto Nacional de Investigaciones Nucleares, Carretera México-Toluca S/N, La Marquesa, Ocoyoacac, Estado de México, C.P. 52750, Mexico. Tel.: +52 55 53297200x3863; fax: +52 55 53297306.
E-mail addresses: ferro_flores@yahoo.com.mx, guillermina.ferro@inin.gob.mx (G. Ferro-Flores).

0378-5173/$ – see front matter © 2009 Elsevier B.V. All rights reserved.
doi:10.1016/j.ijpharm.2009.04.018

ceutical with high stability in human serum, specific cell receptor binding and rapid internalization. Biodistribution data in mice showed rapid blood clearance, with predominant renal excretion and specific binding towards GRP receptor-positive tissues such as pancreas and PC-3 tumors (Ferro-Flores et al., 2006b). Images of GRP-r expression in breast cancer patients demonstrated distinct radioactivity accumulation in malignant tissue (Santos-Cuevas et al., 2008).

Targeted entry into cells is an increasingly important research area. Disease diagnoses and treatment by novel methods would be greatly enhanced by efficiently transporting materials to living cell nuclei. Penetrating peptides are emerging as attractive drug delivery tools. The HIV Tat-derived peptide is a small basic peptide called "trojan horse" for successfully delivering a large variety of cargoes into cells such as nanoparticles, proteins, peptides and nucleic acids. The "transduction domain" or region conveying cell penetrating properties appears to be confined to a small stretch of basic amino acids with the sequence RKKRRQRRR and known as Tat(49–57) (Koch et al., 2003; Dietz and Bähr, 2004; Deshayes et al., 2005; Zhang et al., 2006b; Hu et al., 2007; Jain et al., 2007; Youngblood et al., 2007; Chen and Harrison, 2007; Cornelissen et al., 2008).

Therefore, a new hybrid radiopharmaceutical of type ^{99m}Tc-N_2S_2-Tat(49–57)-Lys^3-bombesin (^{99m}Tc-Tat-BN) would significantly increase cancer cell uptake and consequently image contrast of cancer tumors and their metastases, improving sensitivity and specificity of diagnostic studies in breast cancer.

The aim of this research was to prepare and assess *in vitro* and *in vivo* uptake kinetics in GRP receptor-positive cancer cells of ^{99m}Tc-Tat-BN and to compare its cellular internalization with that of ^{99m}Tc-BN.

2. Experimental

2.1. Design and preparation of hybrid N_2S_2-Tat(49–57)-Lys^3-BN peptide

Tat(49–57) peptide (H-Arg-Lys-Lys-Arg-Arg-Gln-Arg-Arg-Arg-NH_2) was conjugated to Gly-Gly-Cys-Gly-Cys(Acm)-Gly-Cys(Acm)-NH_2 to produce the Tat(49–57)-spacer-N_2S_2 peptide (H-Arg^1-Lys^2-Lys^3-Arg^4-Arg^5-Gln^6-Arg^7-Arg^8-Arg^9-Gly^{10}-Gly^{11}-Cys^{12}-Gly^{13}-Cys^{14}(Acm)-Gly^{15}-Cys^{16}(Acm)-NH_2). The sequence Gly^{13}-Cys^{14}(Acm)-Gly^{15}-Cys^{16}(Acm)-NH_2 was added for use as the specific N_2S_2 chelating site for ^{99m}Tc (Fig. 1).

Lys^3-bombesin (Pyr-Gln-Lys-Leu-Gly-Asn-Gln-Trp-Ala-Vla-Gly-His-Leu-Met-NH_2) was conjugated to maleimidopropyl (MPA) through Lys^3 and the MPA group used as the branch position forming a thioether with the Cys^{12} side chain of Tat(49–57)-spacer-N_2S_2 peptide (Fig. 1). Synthesis, HPLC analysis, Mass Spectral Analysis (MALDI), Amino Acid Analysis (AAA) and peptide content determination were carried out in the Bachem Laboratories obtaining a certified white powder product with chemical purity >90% and molecular weight of 3779.5 g/mol (Bachem, CA, USA).

2.2. Molecular modeling

The N_2S_2-Tat(49–57)-Lys^3-BN peptide molecule was built taking into account valence, bond type, charge and hybridization. The minimum energies (Molecular Mechanics calculations by Augmented MM3 procedure) and the lowest energy conformer (CONFLEX procedure) associated to the optimized geometry of its structure were calculated using the CAChe Pro 5.02 and/or 5.04 program package for windows® (Fujitsu Ltd., 2000–2001). Sequential application of Augmented MM3/CONFLEX procedures yielded the most stable conformers for the N_2S_2-Tat(49–57)-Lys^3-BN and for Tc(O)N_2S_2-Tat(49–57)-Lys^3-BN structures.

2.3. Technetium-99 labeling of N_2S_2-Tat(49–57)-Lys^3-BN

^{99m}Tc-pertechnetate was obtained from a GETEC ^{99}Mo/^{99m}Tc generator (ININ-Mexico). All the other reagents were purchased from Sigma–Aldrich Chemical Co., and used as received.

Acetamidomethyl (Acm) groups deprotection and N_2S_2-Tat(49–57)-Lys^3-bombesin labeling were accomplished in one step by pertechnetate reduction with stannous chloride in ammonium acetate and sodium tartrate presence at room temperature. Alkalinity (pH 9.5) was necessary to de-acetylate Cys^{14}(Acm) and Cys^{16}(Acm) side chains of TAT(49–57)-spacer-N_2S_2 peptide that are essential for oxotechnetate binding (Bogdanov et al., 2001; Zhang et al., 2006a,b).

One milligram of N_2S_2-Tat(49–57)-Lys^3-BN was dissolved in 200 μL of injectable water (Pisa®, Mexico). Ten microliters of this solution were added to 25 μL of sodium ^{99m}Tc-pertechnetate (185 MBq) followed by 7 μL of deprotection mixture (50 mg/mL sodium tartrate in 0.1 M NH_4OH/NH_4CH_3COOH, pH 9.5) and 3 μL of reducing solution (0.5 mg $SnCl_2$/mL in 0.05 M HCl). The final mixture was incubated for 20 min at room temperature.

2.4. Evaluation of ^{99m}Tc-N_2S_2-Tat(49–57)-Lys^3-BN (^{99m}Tc-Tat-BN) radiochemical purity

Radiochemical purity analyses were performed by instant thin-layer chromatography on silica gel (ITLC-SG, Gelman Sciences), solid phase extraction (Sep-Pak C-18 cartridges) and reverse phase high-performance liquid chromatography (HPLC).

ITLC-SG analysis was accomplished using 2 different mobile phases: 2-butanone to determine the amount of free $^{99m}TcO_4^-$ (Rf = 1) and 0.1 M sodium citrate pH 5 to determine ^{99m}Tc-tartrate and $^{99m}TcO_4^-$ (Rf = 1). Rf value of the radiolabeled peptide in each system was 0.0.

The Sep-Pak cartridges were preconditioned with 5 mL of ethanol followed by 5 mL of 1 mM HCl and 5 mL of air. An aliquot of 0.1 mL of the labeled peptide was loaded on the preconditioned Sep-Pak cartridge followed by 5 mL of 1 mM HCl to elute free $^{99m}TcO_4^-$ and ^{99m}Tc-tartrate. The radiolabeled peptide was eluted with 3 mL of ethanol:saline (1:1) mixture and the hydrolyzed-reduced ^{99m}Tc or ^{99m}Tc-colloid remained in the cartridge.

HPLC analyses were carried out with a Waters instrument running Millennium software with both radioactivity and UV-photodiode array in-line detectors and YMC ODS-AQ S5 column (5 μm, 4.6 mm × 250 mm). The gradient was run at a flow rate of 1 mL/min with the following conditions: 0.1% trifluoroacetic acid (TFA)/water (solvent A) and 0.1% TFA/acetonitrile (solvent B). The gradient started with 100% solvent A for 3 min, changed to 50% solvent A over 10 min, was maintained for 10 min, changed to 30% solvent A over 3 min and finally returned to 100% solvent A over 4 min. In this system retention times for free $^{99m}TcO_4^-$, and ^{99m}Tc-Tat-BN were 3–4 min and 10–10.5 min, respectively.

2.5. Serum stability

Size exclusion HPLC analysis and a ITLC-SG were used to estimate serum stability of ^{99m}Tc-Tat-BN. A 50 μL volume of labeled peptide solution (0.5 μg/50 μL) was incubated at 37 °C with 1 mL of fresh human serum. Radiochemical stability was determined from samples of 10 μl taken at different times from 20 min to 24 h for analysis. A shift of the HPLC radioactivity profile to higher molecular weight indicates protein binding, while lower-molecular weight peaks indicate labeled catabolites or serum cysteine binding.

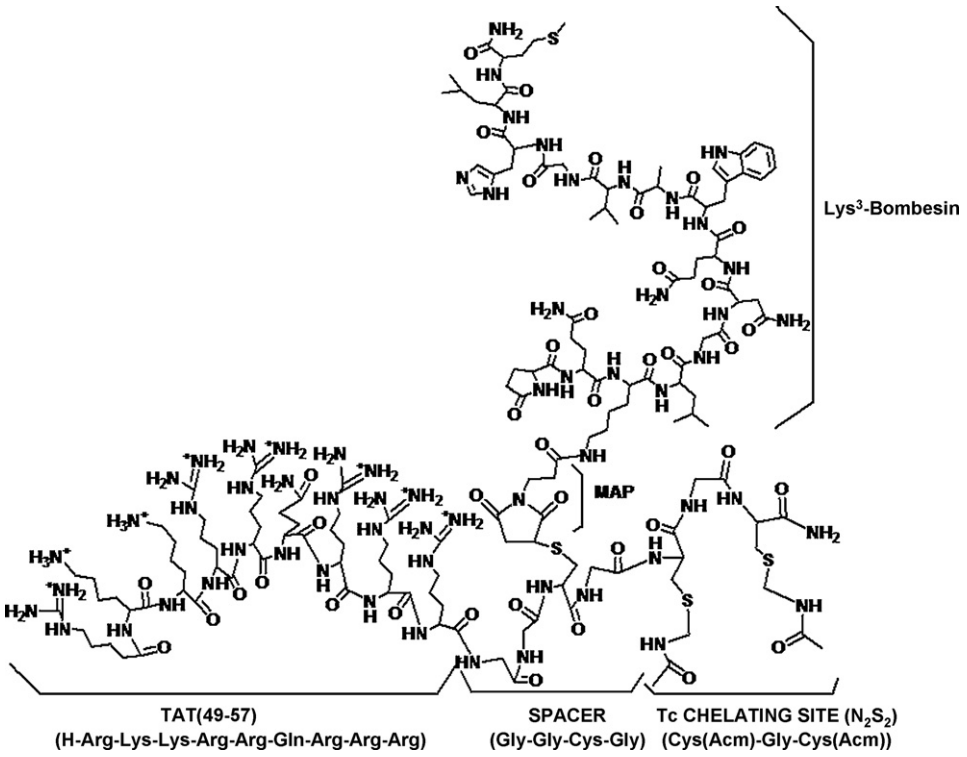

Fig. 1. General scheme of the N_2S_2-Tat(49–57)-Lys^3-BN hybrid peptide.

2.6. Cysteine challenge

^{99m}Tc-Tat-BN was tested for instability towards cysteine. A fresh cysteine solution was prepared (10 mg/mL in 0.1 M PBS, pH 7.0) and diluted to different concentrations. Then 10 μL of each cysteine solution was mixed with 90 μL of 20 μM of the labeled peptide solutions. The molar ratios of cysteine to peptide were 5:1, 50:1 and 500:1. Each test tube was incubated at 37 °C and radiochemical purity analyzed 1 h later by ITLC.

2.7. Preparation of ^{99m}Tc-EDDA/HYNIC-Lys^3-BN (^{99m}Tc-BN)

As previously reported, a lyophilized formulation containing HYNIC-Lys^3-BN, EDDA, tricine, and stannous chloride was prepared (Ferro-Flores et al., 2006b). The radiolabeling procedure was carried out by adding 1 mL of 0.2 M phosphate buffer pH 7.0 to the freeze-dried kit formulation and immediately 740–1110 MBq (1 mL) of ^{99m}Tc-pertechnetate followed by incubation in boiling water for 15 min. Radiochemical purity was also evaluated by reverse phase HPLC and ITLC.

2.8. In vitro kinetic studies

2.8.1. Cell lines

Human prostate cancer cell PC-3 line and human breast carcinoma cell lines MDA-MB231 and MCF7 were originally obtained from ATCC (USA). The cells were routinely grown at 37 °C, with 5% CO_2 atmosphere and 100% humidity in RPMI medium supplemented with 10% newborn calf serum and antibiotics (100 μg/mL streptomycin).

2.8.2. Internalization assay and non-specific binding

PC-3 or MDA-MB231 or MCF7 cells supplied in fresh medium were diluted to 1×10^6 cells/tube and incubated with about 200,000 cpm of ^{99m}Tc-BN (0.3 nmol total peptide) or ^{99m}Tc-Tat-BN (0.3 nmol total bombesin) in triplicate at 37 °C for 0.083, 2, 4, 6 and 24 h. The test tubes were centrifuged (3 min, 500 g), washed twice with phosphate buffer saline (PBS), and the activity of the cell pellet determined in a crystal scintillation well type detector. Radioactivity in the cell pellet represents both externalized peptide (surface bound) and internalized peptide. An aliquot with the initial activity was taken to represent 100%, and the cell uptake activity was then calculated.

The externalized peptide activity was removed with 1 mL of 0.2 M acetic acid/0.5 M NaCl solution added to the resuspended cell pellet. The test tubes were centrifuged, washed with PBS, recentrifuged, and pellet activity was considered as internalization. The cell pellet was re-suspended with 1 M NaOH to break up the membranes, centrifuged and washed with PBS. The supernatant activity represents cytoplasm uptake. Non-specific binding was determined in parallel but in presence of 10 μM Lys^3-BN (Bachem-USA) (blocked receptor cells).

2.8.3. Statistical analysis

Differences between the *in vitro* cell data for BN-radiopharmaceuticals were evaluated with the Student *t*-test.

2.9. Biodistribution studies

Biodistribution and tumor uptake studies in mice were carried out according to the rules and regulations of the Official Mexican Norm 062-ZOO-1999.

Healthy 6-week-old Balb-C mice were used for biodistribution studies. ^{99m}Tc-Tat-BN, 1.11 MBq (30 μCi) in 0.04 mL was injected in a tail vein. The mice ($n = 3$) were sacrificed at 0.25, 05, 2, 4 and 24 h post-injection. Whole heart, lung, liver, spleen, pancreas, kidneys, intestines, muscle, bone and blood samples were saline rinsed, paper blotted and placed into pre-weighed plastic test tubes. The activity was determined in a well-type scintillation detector (*Canberra*) along with six 0.5 mL aliquots of the diluted standard representing 100% of the injected activity. Mean activities were used to

obtain the percentage of injected activity per gram of tissue % IA/g.

2.9.1. Tumor induction in athymic mice

Athymic male mice (20–22 g) were kept in sterile cages with sterile wood-shavings bed, constant temperature, humidity, noise and 12:12 light periods. Water and feed (standard PMI 5001 feed) were given *ad libitum*.

Prostate tumors were induced by subcutaneous injection of PC-3 cells (1×10^6) resuspended in 0.2 mL of phosphate-buffered saline, into the upper back of four 6–7-week-old nude mice. Injection sites were observed at regular intervals for tumor formation and progression.

2.9.2. Imaging

The nude mice with the implanted tumors were sacrificed and scanned with a gamma camera with a pinhole collimator 2 h after ^{99m}Tc-Tat-BN or ^{99m}Tc-BN administration in the tail vein (3 MBq in 0.04 mL). Finally, complete dissection was carried out to determine percentage of injected activity per gram of tissue % IA/g as described above.

3. Results

3.1. Design of $(Acm)_2S_2N_2$-Tat-Lys^3-bombesin and $Tc(O)S_2N_2$-Tat-Lys^3-bombesin by semiempirical calculations

A good molecular modeling yields structures which are similar to those obtained experimentally. However, this similarity could be affected by the size, charge and mobility of the molecule, e.g. in the case of big and charged peptides. Without forgetting this fact, the hybrid N_2S_2-Tat(49–57)-Lys^3-BN peptide (Fig. 2A) was designed using semiempirical calculations to investigate the feasibility of its formation. The minimum energies of its most stable structure and conformer were 271 and 233 kcal/mol, respectively.

The technetium-oxo complex formed with this hybrid peptide was also modeled considering two well-known facts of this type of chelating site: (1) the two terminal thiols $S_2(Acm)_2$ are able to be ionized by removing the acetamidomethyl protecting groups (Canney et al., 1993; Bandoli et al., 2001), (2) the amide groups easily undergo deprotonation (Bandoli et al., 2001). Then it is expected that the chelating site yields a $[N_2S_2]^{4-}$ coordination around the $[Tc(O)]^{3+}$ core forming this way a negative charged five-coordinate complex. Based on the latter, the molecule of the $[TcO(N_2S_2)]^{-1}$-

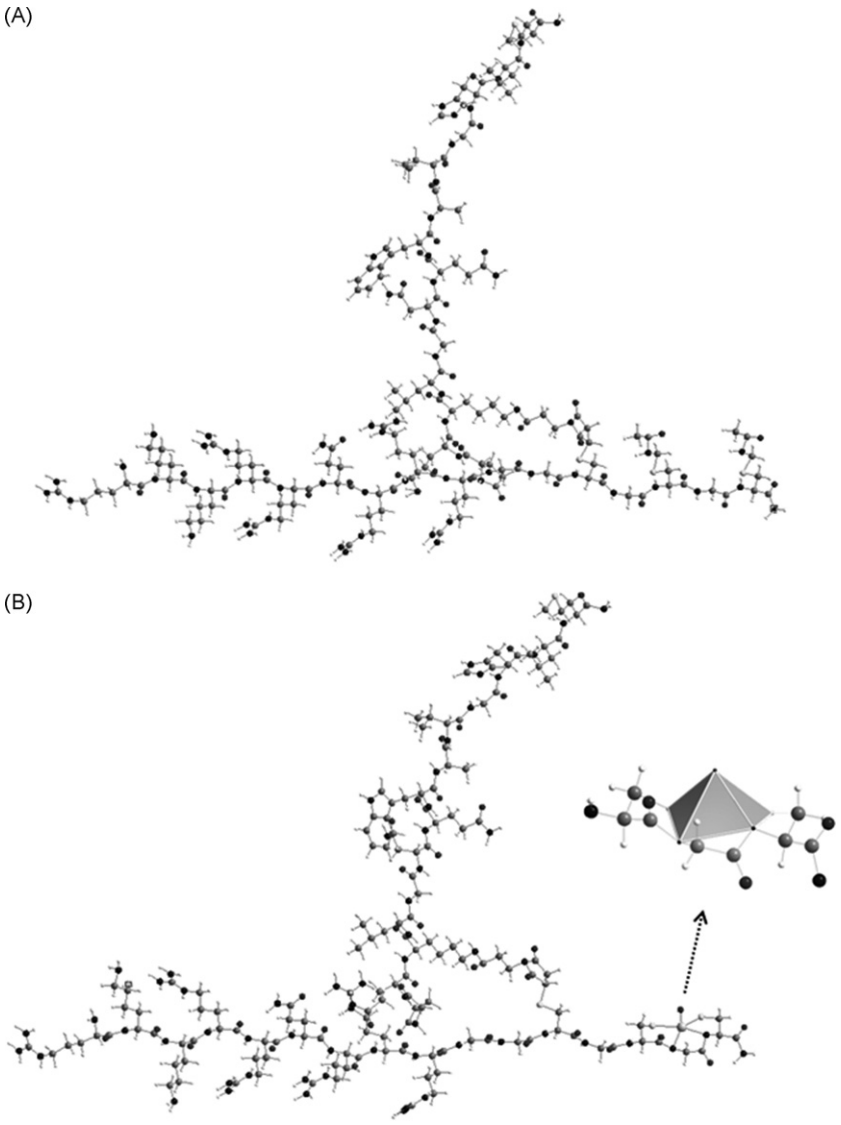

Fig. 2. (A) The most stable conformer of the modeled N_2S_2-Tat(49–57)-Lys^3-BN hybrid peptide molecule using CONFLEX. (B) The most stable conformer of the modeled $Tc(O)N_2S_2$-Tat(49–57)-Lys^3-BN hybrid peptide molecule using CONFLEX. The expanded geometry of the Tc(O) chelate: $[Tc(O)N_2S_2]^{-1}$ is given for clarity.

Table 1
Bond distances of the calculated Tc(O)-N_2S_2-Tat-Lys^3-BN complex using Augmented MM3 and CONFLEX semiempirical procedures.

Compound	Geometry	Bond distances (Å)	Bond distance ratio
$[^{99m}Tc\text{-}(N_2S_2DADS)]^{-1}$	Square pyramid[a]	Tc-N1: 2.002 Tc-N2: 1.984 Tc-S1: 2.300 Tc-S2: 2.286 Tc = O: 1.667	R_N = 1.009 R_S = 1.006 TcN2/TcO = 1.190 TcS1/TcO = 1.38
$[(^{99m}Tc(O)\text{-}(N_2S_2))^{-1}$-Tat-$Lys^3$-BN	Distorted square pyramid	Tc-N1: 2.314 Tc-N2: 2.308 Tc-S1: 2.618 Tc-S2: 2.611 Tc = O: 2.210	R_N = 1.003 R_S = 1.003 TcN2/TcO = 1.04 TcS1/TcO = 1.19

[a] By X-ray diffraction (Canney et al., 1993).

TAT(49–57)-Lys^3-BN peptide complex was calculated (Fig. 2B) using the most stable conformer of the hybrid peptide molecule. The minimum energy of the optimized structure was 300 kcal/mol and that of the most stable conformer equal to 262 kcal/mol. In Table 1 are given some geometrical parameters of this complex.

3.2. Evaluation of ^{99m}Tc-Tat-BN radiochemical purity and stability

The results obtained by ITLC, Sep-Pak and HPLC analyses showed a mean radiochemical purity for ^{99m}Tc-Tat-BN of 92 ± 2% (n > 30) and remains stable after 24 h without post-labeling purification (Fig. 3). The average specific activity was 14 MBq/nmol. After 1 h in human serum the radiochemical purity remained >90% and decreased to 82% and 65% after 3 and 24 h, respectively. Protein binding was 36.4 ± 2.7 at 2 h without ^{99m}Tc transchelation to cysteine (Fig. 4). After incubation with 5:1, 50:1 and 500:1 molar ratios of cysteine to peptide, ITLC analysis revealed that the radioactivity dissociated from ^{99m}Tc-Tat-BN was 7%, 16% and 41%, respectively, indicating adequate radiopharmaceutical stability towards cysteine present in blood.

3.3. In vitro uptake

The *in vitro* results showed an important uptake in the three cancer cell lines PC3, MCF7 and MDA-MB231 which is inhibited significantly by pre-incubation with cold bombesin (Table 2). In general cell binding in blocked cells was less than 3% of total activity for ^{99m}Tc-BN and less than 9% for ^{99m}Tc-Tat-BN in all cell lines and during all times. This confirmed *in vitro* specificity of both radiopharmaceuticals for GRP receptors found in cell membranes of the three cell lines due to the fact that both compounds contain BN. However, the hybrid ^{99m}Tc-Tat-BN shows a higher uptake (p < 0.05) due to Tat's capacity to internalize the molecule into the cytoplasm and even into the nucleus (Costantini et al., 2008).

Internalization increase of ^{99m}Tc-Tat-BN compared with that of ^{99m}Tc-BN in the cell lines is shown in Fig. 5, demonstrating that the hybrid peptide has the ability to penetrate the cell membrane. Maximum internalization is reached in PC3 and MCF7 cells between 2 and 4 h after incubation. However MDA-MB231 cells showed a distinct pattern where cellular internalization reaches a maximum during the first few minutes decreasing with time.

The percentage activity in cytoplasm of the total internal activity (Fig. 6) shows a great difference between both radiopharmaceuticals. Most of ^{99m}Tc-BN remains in the cell membrane while ^{99m}Tc-Tat-BN is released in the cytoplasm, where it can be internalized into the nucleus because of its amino acid nuclear localization sequence (NLS) (Costantini et al., 2008).

3.4. Biodistribution and imaging

^{99m}Tc-Tat-BN biodistribution is shown in Table 3. Renal excretion is predominantly observed but hepatobiliary clearance is also present. GRP-r receptors are naturally expressed in lungs showing radiopharmaceutical uptake (Shriver et al., 2000). However, pancreas shows higher uptake than non-excretory organs such as spleen, muscle and even lungs because of its GRP-r expression, indicating that BN acts as the targeting vector.

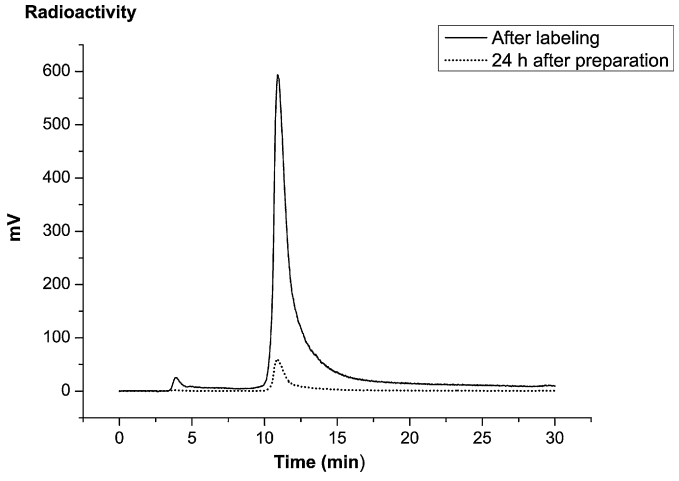

Fig. 3. Reverse phase HPLC radiochromatograms of ^{99m}Tc-N_2S_2-Tat(49–57)-Lys^3-BN after labeling, and 24 h after preparation (kept at room temperature).

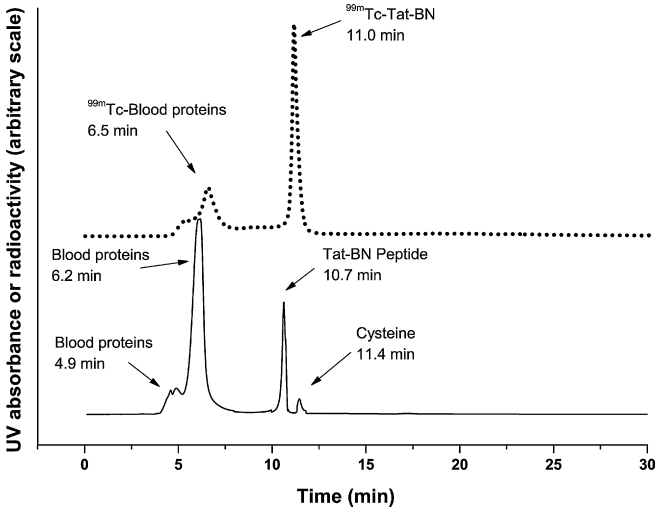

Fig. 4. Size-exclusion HPLC. Solid line represents the UV-chromatogram (280 nm) of human serum proteins and dotted line the radiochromatogram of ^{99m}Tc-N_2S_2-Tat(49–57)-Lys^3-BN 2 h after incubation in human serum at 37 °C.

Table 2
^{99m}Tc-N_2S_2-Tat(49–57)-Lys^3-BN (^{99m}Tc-Tat-BN) and ^{99m}Tc-EDDA/HYNIC-Lys^3-BN (^{99m}Tc-BN) cell uptake in different cancer cell lines (% of total activity ± SD).

Time (h)	PC3		MCF7		MDA-MB231	
	^{99m}Tc-Tat-BN	^{99m}Tc-BN	^{99m}Tc-Tat-BN	^{99m}Tc-BN	^{99m}Tc-Tat-BN	^{99m}Tc-BN
0.083	22.01 ± 2.08	10.29 ± 1.47	19.27 ± 3.55	7.83 ± 0.71	24.33 ± 2.82	5.91 ± 0.26
1	21.43 ± 2.91	8.59 ± 0.59	17.43 ± 1.13	6.79 ± 0.45	19.43 ± 1.30	5.48 ± 0.21
2	24.88 ± 2.12	12.85 ± 0.90	18.27 ± 2.14	8.97 ± 0.92	15.98 ± 1.07	5.06 ± 0.57
4	28.10 ± 3.86	17.62 ± 1.86	13.15 ± 1.27	7.48 ± 0.30	14.40 ± 1.79	4.16 ± 0.39
6	25.43 ± 1.79	9.63 ± 0.47	12.65 ± 0.94	7.98 ± 0.22	13.60 ± 0.96	4.19 ± 0.52
24	23.91 ± 1.53	8.21 ± 0.64	12.30 ± 1.16	2.32 ± 0.49	14.24 ± 0.34	3.43 ± 0.27

Table 3
Biodistribution of ^{99m}Tc-N_2S_2-Tat(49–57)-Lys^3-BN in healthy Balb-C mice at different times after radiopharmaceutical administration (n = 3 in each time).

Tissue	% IA/g (mean ± SD)				
	0.25 h	0.5 h	2 h	4 h	24 h
Blood	7.81 ± 2.62	6.02 ± 2.59	1.12 ± 0.17	1.00 ± 0.03	0.07 ± 0.02
Heart	2.43 ± 0.78	1.62 ± 0.63	0.33 ± 0.07	0.32 ± 0.03	0.09 ± 0.10
Lungs	2.68 ± 0.94	2.26 ± 0.44	0.60 ± 0.08	0.56 ± 0.04	0.09 ± 0.03
Liver	4.91 ± 1.57	3.97 ± 1.70	2.03 ± 0.04	2.11 ± 0.32	0.52 ± 0.17
Spleen	1.28 ± 0.40	0.80 ± 0.30	0.35 ± 0.05	0.55 ± 0.17	0.23 ± 0.07
Pancreas	2.89 ± 1.01	2.65 ± 0.77	1.87 ± 0.11	1.43 ± 0.24	0.21 ± 0.04
Kidneys	16.87 ± 4.85	22.99 ± 8.57	29.02 ± 2.78	27.72 ± 2.18	8.45 ± 0.81
Intestine	3.70 ± 1.49	11.30 ± 7.71	2.06 ± 0.33	2.05 ± 0.98	0.17 ± 0.08
Muscle	1.47 ± 0.26	1.28 ± 0.70	0.58 ± 0.23	0.43 ± 0.14	0.03 ± 0.02
Bone	2.44 ± 0.79	1.74 ± 0.60	0.42 ± 0.05	0.78 ± 0.26	0.19 ± 0.17

Table 4 shows biodistribution in mice with induced PC-3 tumors. Tumor-to-blood, tumor-to-muscle and pancreas-to-blood ratios for ^{99m}Tc-BN were 4.4, 7 and 8.2, respectively, and 3.2, 8 and 1.4 for ^{99m}Tc-Tat-BN correspondingly. *In vivo* images showed a clear tumor uptake and a dissection process to eliminate internal viscera, highlighted the ^{99m}Tc-BN and ^{99m}Tc-Tat-BN uptake in tumor PC-3 cells (Fig. 7). The tumor/muscle ratio obtained from image counts per pixel corresponding to ^{99m}Tc-BN was 7 and for ^{99m}Tc-Tat-BN was 8.5, demonstrating a minimal difference between the two.

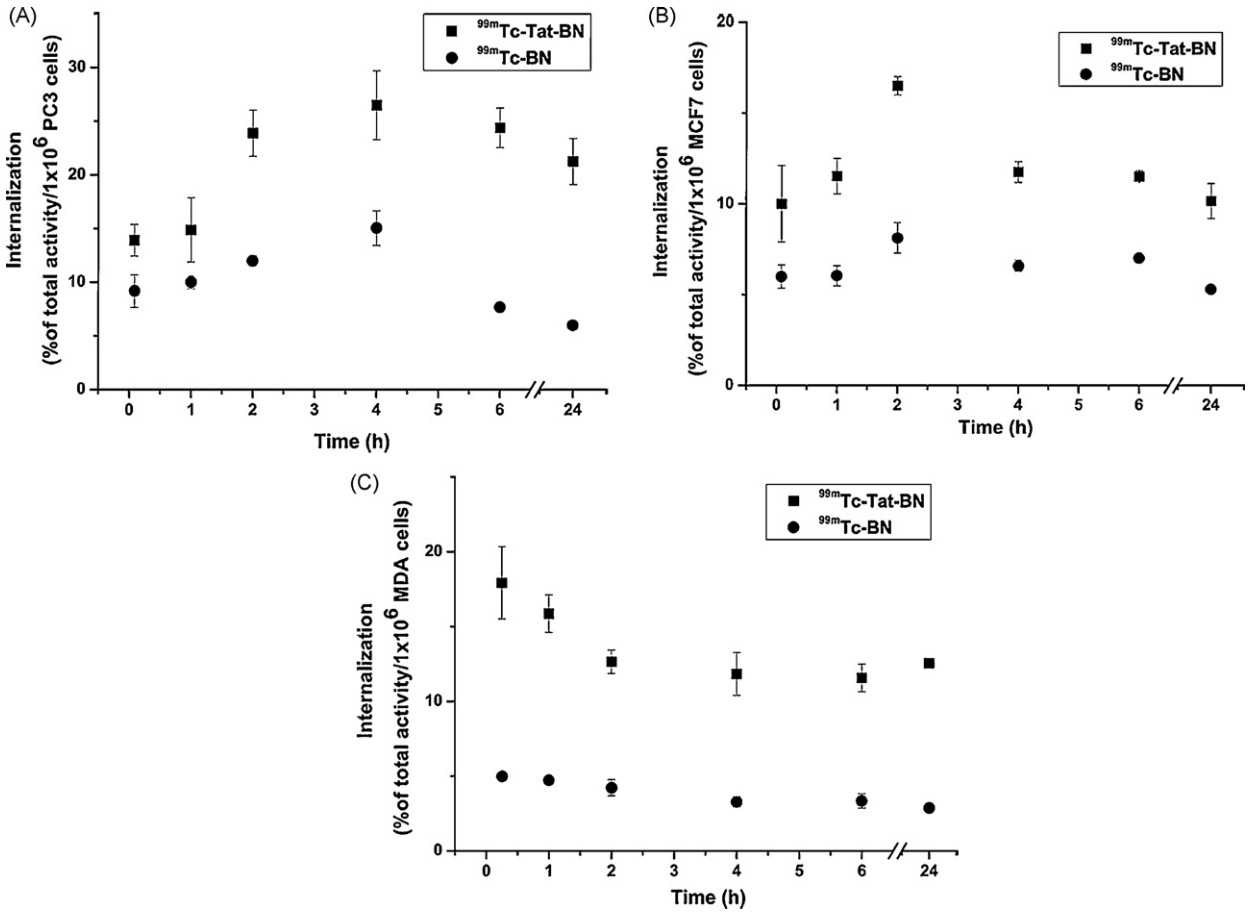

Fig. 5. Time dependent internalization of ^{99m}Tc-N_2S_2-Tat(49–57)-Lys^3-BN (^{99m}Tc-Tat-BN) and ^{99m}Tc-EDDA/HYNIC-Lys^3-BN (^{99m}Tc-BN) in (A) PC3, (B) MCF7 and (C) MDA-MB231 cancer cell lines.

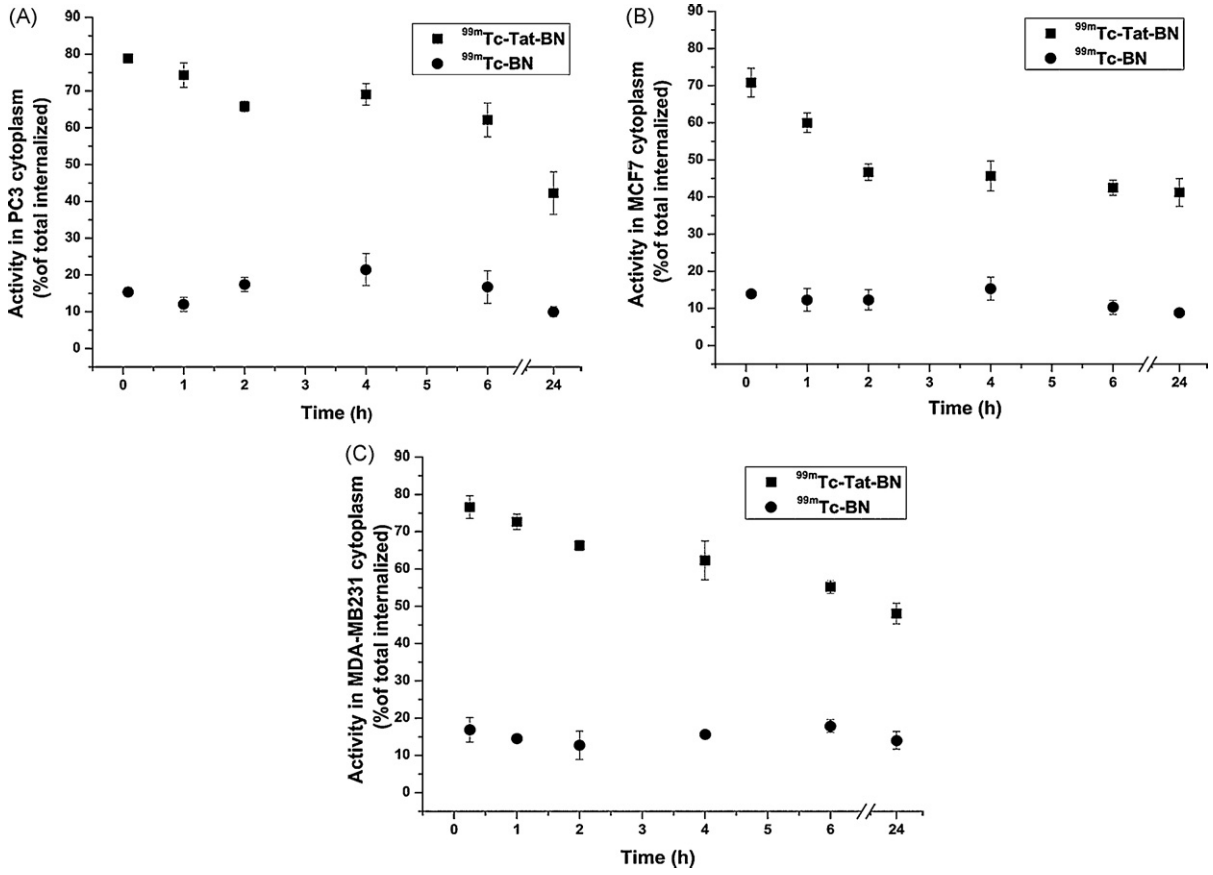

Fig. 6. Uptake of ^{99m}Tc-N_2S_2-Tat(49–57)-Lys^3-BN (^{99m}Tc-Tat-BN) and ^{99m}Tc-EDDA/HYNIC-Lys^3-BN (^{99m}Tc-BN) in the cytoplasm of (A) PC3, (B) MCF7 and (C) MDA-MB231 cancer cell lines.

Table 4
Biodistribution in nude mice with induced PC-3 tumors 2 h after administration of ^{99m}Tc-N_2S_2-Tat(49–57)-Lys^3-BN (^{99m}Tc-Tat-BN) ($n = 3$) or ^{99m}Tc-EDDA/HYNIC-Lys^3-BN (^{99m}Tc-BN) ($n = 3$).

Tissue	% IA/g (mean ± SD)	
	^{99m}Tc-BN	^{99m}Tc-Tat-BN
Blood	0.40 ± 0.03	1.22 ± 0.16
Heart	0.25 ± 0.02	0.43 ± 0.08
Lung	0.50 ± 0.04	0.54 ± 0.07
Liver	0.85 ± 0.04	2.14 ± 0.05
Spleen	0.40 ± 0.05	0.42 ± 0.04
Pancreas	3.29 ± 0.21	1.69 ± 0.12
Kidney	23.5 ± 1.21	28.12 ± 2.18
Intestine	0.85 ± 0.13	1.96 ± 0.23
Muscle	0.25 ± 0.03	0.48 ± 0.05
Tumor	1.75 ± 0.11	3.84 ± 0.25

4. Discussion

The minimum energies of the calculated hybrid peptide are adequate for its molecular structure since the large size, complexity and high charge of this peptide impose steric and electrostatic repulsions against its stabilization at lower minimum energies. However, the comparison of its minimum energy (271 kcal/mol) to those reported for other calculated structures of smaller charged peptides like UBI(29–41) (Melendez-Alafort et al., 2003), Tat-Scr (Ferro-Flores et al., 2004), 90 and 72–90 kcal/mol, respectively, suggested that the hybrid peptide has to be stable. In addition, the conformation acquired by the peptide molecule does not interfere with the recognition capability of BN. These facts supported the proposal that the preparation of the hybrid peptide has to be viable and the specificity maintained.

$[TcO(N_2S_2)]^{-1}$-Tat(49–57)-Lys^3-BN peptide structure acquired in the chelating site a distorted square pyramidal geometry with the oxo group at the apical position of the pyramid and Tc about the center of the plane formed by the N_2S_2 donors (see expanded segment of the molecule, Fig. 2B). This geometry has been found by X-ray diffraction for other five-coordinate Tc(O) complexes neutral or charged compounds like negatively charged five coordinate $Tc(O)N_2S_2$ complexes (Bandoli et al., 2001; Canney et al., 1993). The minimum energy of this complex does not differ significantly from that of the hybrid peptide before coordination to $[Tc(O)]^{3+}$. This evidence together the geometrical arrangement acquired by the complexed hybrid peptide (Fig. 2B) demonstrate that the recognition capability of the peptide is little affected by the formation of the $Tc(O)N_2S_2$ complex. However, the stability of the $[Tc(O)(N_2S_2)]^{-1}$ chelate itself could be affected.

In general ^{99m}Tc-Tat-BN did not show the excellent radiochemical characteristics as that previously reported for ^{99m}Tc-BN (Ferro-Flores et al., 2006b), since the first one showed slightly lower radiochemical purity (>95% for ^{99m}Tc-BN) and lower stability in cysteine and human serum. These results were expected since HYNIC core with additional co-ligands has demonstrated to be highly stable for labeling peptides (Liu and Edwards, 1999; Decristoforo et al., 2000). Nevertheless, the technetium-binding region consisting of Gly-Gly-Cys-NH_2 or Cys-Gly-Cys-NH_2 peptide (to form a $-N_2S_2-$ or $-N_3S-$ ligand) has been successfully used to prepare stable complexes with the $Tc=O^{3+}$ core producing minimum alteration of the molecule bioactivity in agreement with results obtained in this research (Bogdanov et al., 2001; Francesconi et al., 2004; Zhang et al., 2006b).

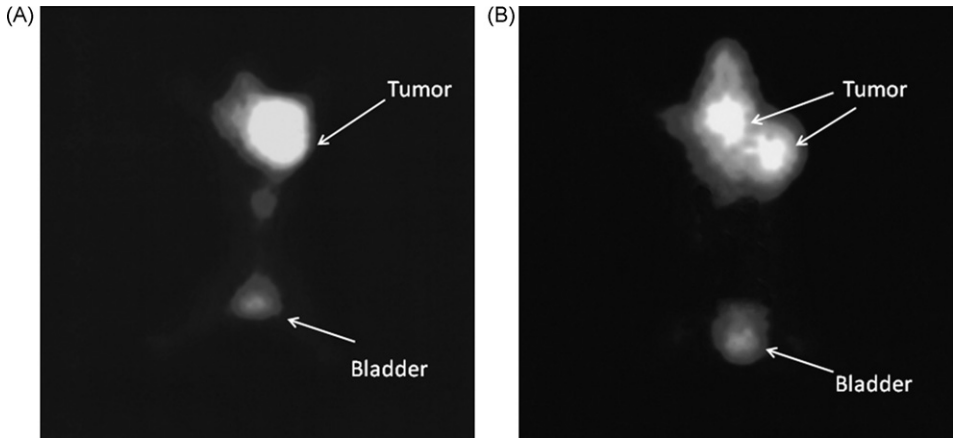

Fig. 7. Uptake of (A) ^{99m}Tc-N_2S_2-Tat(49–57)-Lys^3-BN (^{99m}Tc-Tat-BN) and (B) ^{99m}Tc-EDDA/HYNIC-Lys^3-BN (^{99m}Tc-BN) in tumor PC3 cells in athymic mouse 2 h after radiopharmaceutical administration (mice with dissection of internal viscera to highlight tumor uptake).

^{99m}Tc-Tat-BN binds to plasmatic proteins approximately 20% more than ^{99m}Tc-BN. These data indicate that in spite of the fact that both radiopharmaceuticals contain BN and are labeled with ^{99m}Tc, the positive charges of Tat due to arginines and lysines contained in its amino acid sequence, tend to interact faster and in a strong way with proteins, besides that it is not targeted to a specific receptor (Costantini et al., 2008; Cornelissen et al., 2008). This cationic property is necessary to penetrate the cell membrane and localize the nucleus (Drin et al., 2003), but these characteristics can have an effect in blood elimination rate by binding to plasmatic proteins as well as increasing interaction and internalization in cells and healthy tissue (e.g. plasmatic cells, spleen and liver). Although cancer cell uptake was significantly higher for ^{99m}Tc-Tat-BN with respect to ^{99m}Tc-BN, the higher activity in blood for the first one did not produce a very high increase in the contrast of tumor image in mice (Fig. 7).

The maximum uptake of both radiopharmaceuticals was presented at the same times in all cancer cells, in PC3 at 4 h (^{99m}Tc-BN, $17.62 \pm 1.86\%$; ^{99m}Tc-Tat-BN, $28.1 \pm 2.86\%$), in MCF7 at 2 h (^{99m}Tc-BN, $8.97 \pm 0.92\%$; ^{99m}Tc-Tat-BN, $18.27 \pm 2.14\%$) and in MDA-MB231 at 5 min (^{99m}Tc-BN, $5.91 \pm 0.26\%$; ^{99m}Tc-Tat-BN, $24.33 \pm 2.82\%$) with differences only attributed to GRP-r cell expression. In this point it is important to mention that although MCF7 and MDA-MB231 are both breast cancer cell lines, the first one is estrogen-dependent and the latter is estrogen-independent, and it has been suggested that the GRP-r expression is estrogen-dependent in the early stages of breast carcinoma (Halmos et al., 1995). The elimination of the radiopharmaceuticals in the following times is due to the fact that the internalization process of the ligand/GRP-r complex involves lysosomes final trapping upon binding, where, in the case of the peptides, are quickly degraded. Due to this immediate lysosome degradation, no radioactivity accumulation in cells was expected (La Bella et al., 2002).

Receptor proteins in cells are considered targets in molecular nuclear medicine. In general cell internalization was receptor specific with ^{99m}Tc-BN and in the ^{99m}Tc-Tat-BN case 9% of total activity was non-specific as demonstrated uptake results in GRP-r blocked cell experiments because of Tat nuclear localizing sequence (NLS) (Costantini et al., 2008).

In this work the nucleus of the cytoplasm was not separated to quantify nuclear internalization. Nevertheless it was considered necessary to carry out this test with the purpose of estimating cellular dosimetry because of ^{99m}Tc-auger electron emission.

Biodistribution studies showed a slow blood clearance for ^{99m}Tc-Tat-BN, the contrary was observed in non-target organs, however, maximum uptake was observed in kidneys indicating principal renal excretion. These results coincide with ^{99m}Tc-BN biodistribution studies where excretion is mainly renal and uptake in non-target organs was lower with faster blood clearance. Nevertheless both radiopharmaceuticals showed good tumor localization for PC3 cells in athymic mice. However ^{99m}Tc-Tat-BN showed a slightly better tumor/muscle ratio of 8.5 compared to 7 for ^{99m}Tc-BN.

High ^{99m}Tc-Tat-BN uptake in kidneys and in non-target organs shows the need for an improved method for reducing radioactivity background which could be done by the co-administration of a cold lysine–arginine infusion as previously reported for other peptide-radiopharmaceuticals (Bodei et al., 2003).

5. Conclusions

^{99m}Tc-N_2S_2-Tat(49–57)-Lys^3-BN has been developed as a hybrid radiopharmaceutical composed of a penetrating peptide with specific targeting moiety (Tat conjugated to BN) producing a stable labeled molecule able to overcome the lypophilic cell membrane barrier with higher internalization in GRP-receptor positive cancer cells with respect to ^{99m}Tc-EDDA/HYNIC-Lys^3-BN. Therefore, this hybrid is potentially useful in breast and prostate cancer imaging.

Acknowledgements

This study was supported by the CONACyT-SALUD-69051-Mexico and the International Atomic Energy Agency (Contract No. 14539/RO).

References

Alves, S., Correia, J.D., Santos, I., Veerendra, B., Sieckman, G.L., Hoffman, T.J., Rold, T.L., Figueroa, S.D., Retzloff, L., McCrate, J., Prasanphanich, A., Smith, C.J., 2006. Pyrazolyl conjugates of bombesin: a new tridentate ligand framework for the stabilization of fac-$[M(CO)_3]^+$ moiety. Nucl. Med. Biol. 33, 625–634.

Baidoo, K.E., Lin, K.S., Zhan, Y., Finley, P., Scheffel, U., Wagner, H.N., 1998. Design, synthesis, and initial evaluation of high-affinity technetium bombesin analogues. Bioconjugate Chem. 9, 218–225.

Bandoli, G., Dolmella, A., Porchia, M., Refosco, F., Tisato, F., 2001. Structural overview of technetium compounds (1993–1999). Coord. Chem. Rev. 214, 43–90.

Bodei, L., Cremonesi, M., Zoboli, S., Grana, C., Bartolomei, M., Rocca, P., Caracciolo, M., Macke, H.R., Chinol, M., Paganelli, G., 2003. Receptor-mediated radionuclide therapy with ^{90}Y-DOTATOC in association with amino acid infusion: a phase 1 study. Eur. J. Nucl. Med. 30, 207–216.

Bogdanov, A., Tung, C.-H., Bredow, S., Weissleder, R., 2001. DNA binding chelates for nonviral gene delivery imaging. Gene Ther. 8, 515–522.

Canney, D.J., Billings, J., Francesconi, L.C., Guo, Y.-Z., Haggerty, B.S., Rheingold, A.L., Kung, H.F., 1993. Dicarboxylate diamide dimercaptide (N_2S_2) technetium-99m complexes: synthesis and biological evaluation as potential renal radiopharmaceuticals. J. Med. Chem. 36, 1032–1040.

Chen, L., Harrison, S.D., 2007. Cell-penetrating peptides in drug development: enabling intracellular targets. Biochem. Soc. Trans. 35, 821–825.
Cornelissen, B., McLarty, K., Kersemans, V., Scollard, D., Reilly, R., 2008. Properties of [^{111}In]-labeled HIV-1 tat peptide radioimmunoconjugates in tumor-bearing mice following intravenous or intratumoral injection. Nucl. Med. Biol. 35, 101–110.
Costantini, D.L., Hu, M., Reilly, R., 2008. Peptide motifs for insertion of radiolabeled biomolecules into cells and routing to the nucleus for cancer imaging or radiotherapeutic applications. Cancer Biother. Radiopharm. 23, 3–23.
Decristoforo, C., Melendez-Alafort, L., Sosabowski, J.K., Mather, S.J., 2000. ^{99m}Tc-HYNIC-[Tyr^3]-octreotide for imaging somatostatin-receptor-positive tumors: preclinical evaluation and comparison with ^{111}In-octreotide. J. Nucl. Med. 41, 1114–1119.
Deshayes, S., Morris, M.C., Divita, G., Heitz, F., 2005. Interactions of primary amphipathic cell penetrating peptides with model membranes: consequences on the mechanisms of intracellular delivery of therapeutics. Curr. Pharm. Des. 11, 3629–3638.
de Visser, M., Verwijnen, S.M., de Jong, M., 2008. Improvement strategies for peptide receptor scintigraphy and radionuclide therapy. Cancer Biother. Radiopharm. 23, 137–157.
Dietz, G.P., Bähr, M., 2004. Delivery of bioactive molecules into the cell: the Trojan horse approach. Mol. Cell. Neurosci. 27, 85–131.
Drin, G., Cottin, S., Blanc, E., Rees, A., Temsamani, J., 2003. Studies on the internalization mechanism of cationic cell penetrating peptides. J. Biol. Chem. 278, 31192–31201.
Faintuch, B.L., Santos, R.L.S., Souza, A.L.F., Hoffman, J., Greeley, M., Smith, C.J., 2005. ^{99m}Tc-Hynic-bombesin (7–14)NH_2: radiochemical evaluation with coligands EDDA (EDDA = ethylenediamine-N,N′-diacetic acid), tricine and nicotinic acid. Synth. React. Inorg. Met.-Org. Nano-Met. Chem. 16, 438–442.
Ferro-Flores, G., de Ramírez, F.M., Meléndez-Alafort, L.G., Arteaga de Murphy, C., Pedraza-López, M., 2004. Molecular recognition and stability of ^{99m}Tc-UBI 29-41 based on experimental and semiempirical results. Appl. Radiat. Isot. 61, 1261–1268.
Ferro-Flores, G., Arteaga de Murphy, C., Melendez-Alafort, L., 2006a. Third generation radiopharmaceuticals for imaging and targeted therapy. Curr. Pharm. Anal. 2, 339–352.
Ferro-Flores, G., Arteaga de Murphy, C., Rodriguez-Cortes, J., Pedraza-Lopez, M., Ramirez-Iglesias, M.T., 2006b. Preparation and evaluation of ^{99m}Tc-EDDA/HYNIC-[Lys^3]-bombesin for imaging of GRP receptor-positive tumours. Nucl. Med. Commun. 27, 371–376.
Francesconi, L.C., Zheng, Y., Bartis, J., Blumenstein, M., Costello, C., De Rosch, M.A., 2004. Preparation and characterization of [^{99}TcO] apcitide: a technetium labeled peptide. Inorg. Chem. 43, 2867–2875.
Garcia-Garayoa, E., Ruegg, D., Blauenstein, P., Zwimpfer, M., Khan, I.U., Maes, V., Blanc, A., Beck-Sickinger, A.G., Tourwe, D.A., Schubiger, P.A., 2007. Chemical and biological characterization of new $Re(CO)_3$/[^{99m}Tc]$(CO)_3$ bombesin analogues. Nucl. Med. Biol. 34, 17–28.
Halmos, G., Wittliff, J.L., Schally, A.V., 1995. Characterization of bombesin/gastrin releasing peptide receptors in human breast cancer and their relationship to steroid receptor expression. Cancer Res. 55, 280–287.
Hu, M., Chen, P., Wang, J., Scollard, D.A., Vallis, K.A., Reilly, R.M., 2007. ^{123}I-labeled HIV-1 tat peptide radioimmuno conjugates are imported into the nucleus of human breast cancer cells and functionally interact in vitro and in vivo with the cyclin-dependent kinase inhibitor, p21(WAF-1/Cip-1). Eur. J. Nucl. Med. Mol. Imaging 34, 368–377.
Jain, M., Venkatraman, G., Batra, S.K., 2007. Cell-penetrating peptides and antibodies: a new direction for optimizing radioimmunotherapy. Eur. J. Nucl. Med. Mol. Imaging 34, 973–977.
Koch, A.M., Reynolds, F., Kircher, M.F., Merkle, H.P., Weissleder, R., Josephson, L., 2003. Uptake and metabolism of a dual fluorochrome Tat-nanoparticle in HeLa cells. Bioconjugate Chem. 14, 115–1121.
Kunstler, J.U., Veerendra, B., Figueroa, S.D., Sieckman, G.L., Rold, T.L., Hoffman, T.J., Smith, C.J., Pietzsch, H.J., 2007. Organometallic (99m)Tc(III) '4+1' Bombesin(7–14) conjugates: synthesis, radiolabeling, and in vitro/in vivo studies. Bioconjugate Chem. 18, 1651–1716.
La Bella, R., Garcia-Garayoa, E., Langer, M., Blauenstein, P., Beck-Sickinger, A.G., Schubiger, A., 2002. In vitro and in vivo evaluation of a ^{99m}Tc(1)-labeled bombesin analogue for imaging of gastrin releasing peptide receptor-positive tumors. Nucl. Med. Biol. 29, 553–560.
Lin, K.S., Liu, A., Baidoo, K.E., Hashemzadeh-Gargari, H., Chen, M.K., Brenneman, K., Pili, R., Pomper, M., Carducci, M.A., Wagner, H.N., 2005. A new high affinity technetium-99m-bombesin analogue with low abdominal accumulation. Bioconjugate Chem. 16, 43–50.
Liu, S., Edwards, D.S., 1999. ^{99m}Tc-labelled small peptides as diagnostic radiopharmaceuticals. Chem. Rev. 99, 2235–2251.
Lui, V.W., Thomas, S.M., Zhang, Q., Wentzel, A.L., Siegfried, J.M., Li, J.Y., Grandis, J.R., 2003. Mitogenic effects of gastrin-releasing peptide in head and neck squamous cancer cells are mediated by activation of the epidermal growth factor receptor. Oncogene 22, 6183–6193.
Melendez-Alafort, L., Ramirez, F., de, M., Ferro-Flores, G., Arteaga de Murphy, C., Pedraza-Lopez, M., Hnatowich, D.J., 2003. Lys and Arg in UBI: a specific site for a stable Tc-99m complex? Nucl. Med. Biol. 30, 605–615.
Nock, B.A., Nikolopoulou, A., Galanis, A., Cordopatis, P., Waser, B., Reubi, J.C., Maina, T., 2005. Potent bombesin-like peptides for GRP-receptor targeting of tumors with ^{99m}Tc: a preclinical study. J. Med. Chem. 48, 100–110.
Reubi, J.C., 2003. Peptide receptors as molecular targets for cancer diagnosis and therapy. Endocrine Rev. 24, 389–427.
Santos-Cuevas, C.L., Ferro-Flores, G., Arteaga de Murphy, C., Pichardo-Romero, P., 2008. Targeted imaging of GRP receptors with ^{99m}Tc-EDDA/HYNIC-[Lys^3]-bombesin: biokinetics and dosimetry in women. Nucl. Med. Commun. 29, 741–747.
Shriver, S.P., Bourdeau, H.A., Gubish, C.T., Tirpak, D.L., Davis, A.L., Luketich, J.D., Siegfried, J.M., 2000. Sex-specific expression of gastrin-releasing peptide receptor: relationship to smoking history and risk of lung cancer. J. Natl. Cancer Inst. 92, 24–33.
Smith, C.J., Sieckman, G.L., Owen, N.K., Hayes, D.L., Mazuru, D.G., Volkert, W.A., Hoffman, T.J., 2003. Radiochemical investigations of [$^{188}Re(H_2O)(CO)_3$-diaminopropionic acid-SSS-bombesin(7–14)NH_2]: synthesis, radiolabeling and in vitro/in vivo GRP receptor targeting studies. Anticancer Res. 23, 63–70.
Thakur, M., Lentle, B.C., 2005. Report of a summit on molecular imaging. Radiology 236, 753–755.
Varvarigou, A., Scopinaro, F., Leondiadis, L., Corleto, V., Schillaci, O., de Vincentis, G., 2002. Synthesis, chemical, radiochemical and radiobiological evaluation of a new ^{99m}Tc-labeled bombesin-like peptide. Cancer Biother. Radiopharm. 17, 317–326.
Youngblood, D.S., Hatlevig, S.A., Hassinger, J.N., Iversen, P.L., Moulton, H.M., 2007. Stability of cell-penetrating peptide-morpholino oligomer conjugates in human serum and in cells. Bioconjugate Chem. 18, 50–60.
Zhang, X., Cai, W., Cao, F., Schreibmann, E., Wu, Y., Wu, J.C., Xing, L., Chen, X., 2006a. ^{18}F-labeled bombesin analogs for targeting GRP receptor-expressing prostate cancer. J. Nucl. Med. 47, 492–501.
Zhang, Y.-M., Tung, C.H., He, J., Liu, N., Yanachkov, I., Liu, G., Rusckowski, M., Vanderheyden, J.L., 2006b. Construction of a novel chimera consisting of a chelator-containing Tat peptide conjugated to a morpholino antisense oligomer for technetium-99m labeling and accelerating cellular kinetics. Nucl. Med. Biol. 33, 263–269.